Molecular Genetic Characterization of Six Recessive Viable Alleles of the Mouse *agouti* Locus

Carolyn M. Hustad,* William L. Perry,* Linda D. Siracusa,*,[1] Carol Rasberry,[†] Leon Cobb,[†] Bruce M. Cattanach,[†] Robert Kovatch,[‡] Neal G. Copeland* and Nancy A. Jenkins*

**Mammalian Genetics Laboratory, ABL-Basic Research Program, NCI-Frederick Cancer Research and Development Center, Frederick, Maryland 21702, [†]Genetics Division, MRC Radiobiology Unit, Chilton, Didcot, Oxon OX11 ORD, United Kingdom, and [‡]Pathology Associates, Inc., Wormans Mill Court, Frederick, Maryland 21701*

Manuscript received December 21, 1994
Accepted for publication January 30, 1995

ABSTRACT

The *agouti* locus on mouse chromosome 2 encodes a secreted cysteine-rich protein of 131 amino acids that acts as a molecular switch to instruct the melanocyte to make either yellow pigment (phaeomelanin) or black pigment (eumelanin). Mutations that up-regulate *agouti* expression are dominant to those causing decreased expression and result in yellow coat color. Other associated effects are obesity, diabetes, and increased susceptibility to tumors. To try to define important functional domains of the agouti protein, we have analyzed the molecular defects present in a series of recessive viable *agouti* mutations. In total, six alleles (a^{mJ}, a^{u}, a^{da}, a^{16H}, a^{18H}, a^{e}) were examined at both the RNA and DNA level. Two of the alleles, a^{16H} and a^{e}, result from mutations in the *agouti* coding region. Four alleles (a^{mJ}, a^{u}, a^{18H}, and a^{da}) appear to represent regulatory mutations that down-regulate *agouti* expression. Interestingly, one of these mutations, a^{18H}, also appears to cause an immunological defect in the homozygous condition. This immunological defect is somewhat analogous to that observed in *motheaten* (*me*) mutant mice. Short and long-range restriction enzyme analyses of homozygous a^{18H} DNA are consistent with the hypothesis that a^{18H} results from a paracentric inversion where one end of the inversion maps in the 5′ regulatory region of *agouti* and the other end in or near a gene that is required for normal immunological function. Cloning the breakpoints of this putative inversion should allow us to identify the gene that confers this interesting immunological disorder.

MUTATIONS at the *agouti* locus on mouse chromosome 2 result in a wide variety of coat color alterations. The agouti protein induces the production of phaeomelanin (yellow pigment) by melanocytes and so determines the amount of yellow present in the hair shaft. Wild-type *agouti* mice have coats composed of hairs with a characteristic banding pattern of black at the base of the hair shaft, a yellow band near the top, and black at the tip (SILVERS 1979). More than 25 alleles or pseudoalleles of *agouti* have been described (SILVERS 1979; CATTANACH *et al.* 1987; GREEN 1989). Alleles causing ectopic expression of the agouti protein are dominant to those causing decreased expression and result in mice with yellow coats and other pleiotropic effects such as obesity and diabetes (HELLERSTRÖM and HELLMAN 1963; DICKIE 1969; COLEMAN 1982; FRIGERI *et al.* 1988; MICHAUD *et al.* 1994b; YEN *et al.* 1994) and an increased susceptibility to certain tumors (HESTON and VLAHAKIS 1961, 1968; YEN *et al.* 1994). Conversely, recessive *agouti* mutations give rise to animals with darker than normal coats. With the recent cloning of the *agouti* gene (BULTMAN *et al.* 1992; MILLER *et al.* 1993), the molecular nature of the large number of *agouti* alleles displaying a variety of phenotypes can now be studied.

The *agouti* transcript is 0.8 kb and contains four exons: exons 2–4 contain the coding region and exon 1 is untranslated. Four separate exon 1 regions have been identified: exon 1A and exon 1A′, located ~120 kb upstream of the coding region and present only in *agouti* mRNA from ventral skin; and the hair growth cycle-specific exons 1B and 1C, which are separated by 40 nt and located 18 kb upstream of the coding region (BULTMAN *et al.* 1994; SIRACUSA 1994; VRIELING *et al.* 1994). The product of the *agouti* locus is a cysteine-rich 131 amino acid protein that is not expressed by melanocytes, but by other cells of the hair follicle. While it is known that the agouti protein regulates phaeomelanin production, its mechanism of action is still under investigation.

Several of the dominant *agouti* alleles have been examined at the molecular level and are found to be due to regulatory mutations. Ectopic expression of *agouti* in these mutants is due to either a large deletion that causes the gene to come under the regulation of an ubiquitous promoter (BULTMAN *et al.* 1992; MICHAUD *et al.* 1993; MILLER *et al.* 1993; DUHL *et al.* 1994a) or to

Corresponding author: Nancy A. Jenkins, Mammalian Genetics Laboratory, NCI-Frederick Cancer Research and Development Center, P.O. Box B, Frederick, MD 21702.

[1] *Present address*: Jefferson Cancer Institute, Thomas Jefferson University, Department of Microbiology and Immunology, 233 South 10th St., Philadelphia, PA 19107.

the insertion of intracisternal A-particle (IAP) elements or novel sequences upstream of the coding region (DUHL *et al.* 1994b; MICHAUD *et al.* 1994a). Because analysis of the dominant alleles did not shed light on which regions of the agouti protein are necessary for proper phaeomelanin production, we have examined six recessive viable *agouti* mutations to find clues to the functional domains of the protein. Two other recessive alleles [*nonagouti* (*a/a*) and *black-and-tan* (*a^t*)] have recently been characterized and found to result from promoter and regulatory mutations (BULTMAN *et al.* 1994). To determine the alterations responsible for the six recessive phenotypes examined here, we have analyzed both the structure and expression of *agouti* in the mutants. Interestingly, one of these mutants, *a^{18H}*, has an immune disorder as well as a darker coat. Because *a^{18H}* is the only *agouti* recessive mutation to display an immune disease phenotype, it is unlikely that a simple mutation in the *agouti* locus is responsible for both the coat color change and the immunological defect. Here we present our initial characterization of the putative chromosomal rearrangement associated with the *a^{18H}* allele.

MATERIALS AND METHODS

Mice: Six viable recessive *agouti* alleles were analyzed in this study. *Nonagouti mottled-JAX* (*a^{mJ}*) mice have a phenotype ranging from agouti to completely black. This mutation arose spontaneously on a (C3H/HeJ × C57BL/6J) F_1 background. All of the Harwell mutations (*a^u*, *a^{da}*, *a^{16H}*, *a^{18H}*) were induced in specific locus mutation experiments. Thus, male (C3H/HeH × 101/H) F_1 hybrid mice were mutagenized and mated to tester females homozygous for seven recessive mutations (*a*, *b*, *p*, *c^{ch}*, *se*, *d*, *s*). The progeny of this cross were screened for mutations at each of these loci. Unless otherwise stated, radiation was the mutagen used. *Agouti umbrous* (*a^u*) mice are characterized by a dark agouti dorsum and ventrum as well as dark agouti pinna hairs (PHILLIPS 1959; CATTANACH *et al.* 1987). Mice that are *nonagouti with dark agouti belly* (*a^{da}*) can be either nonagouti, with nonbanded black hairs and yellow pinna hairs, or can have an extreme umbrous back, a dark agouti belly, and yellow pinna hairs (PHILLIPS 1976; CATTANACH *et al.* 1987). An ethylnitrosourea (ENU) mutant, *nonagouti-16H* (*a^{16H}*), has a dark dorsum, dark agouti sides, and a lighter belly (LYON *et al.* 1985). Although homozygotes died prenatally on the original background (LYON *et al.* 1985), this lethality (but not the coat color change) was lost when the *a^{16H}* mutation was moved onto the C57BL/6J background (L. D. SIRACUSA, unpublished data; MILLER *et al.* 1994). *Nonagouti-18H* (*a^{18H}*) heterozygous mice have a dark band down the back, while homozygous mice have black pinna hairs and are a uniform dark agouti color (CATTANACH *et al.* 1987). *Extreme nonagouti* (*a^e*), the most severe of the recessive viable *agouti* alleles, is a radiation-induced mutation on an S strain background. These mice are completely black, including the pinna hairs (HOLLANDER and GOWEN 1956). All of these mutations were made congenic on the C57BL/6J background. The mutant mouse strain JU/Ct-*a,c-a18H/a18H* was maintained and propagated at the MRC Radiobiology Unit, Chilton, Didcot, Oxon, UK. The mutant mouse strains C57BL/6J-*a^{mJ}/a^{mJ}* ($N_{11}F_6$), C57BL/6J-*a^u/a^u* ($N_{14}F_7$), C57BL/6J-*a^{da}/a^{da}* ($N_{16}F_8$), C57BL/6J-*a^e/a^e* ($N_{12}F_{20}$), C57BL/6J-*a^{16H}/a^{16H}* (N_8F_{12}) and C57BL/6J-*a^{18H}/a18H* (N_6F_8) were maintained and propagated in the Mammalian Genetics Laboratory, ABL-Basic Research Program, Frederick, MD.

RNA extractions: Total cellular RNA was isolated from 4–5-day-old mouse skin according to a procedure adapted from CHIRGWIN *et al.* (1979) and SAMBROOK *et al.* (1989). Tissues were quick frozen in liquid nitrogen and stored at −80° until needed. Samples were homogenized with a Polytron tissue homogenizer (Brinkmann Instruments, Westbury, NY) at room temperature in a homogenization buffer containing 4 M guanidine thiocyanate and centrifuged through a cesium chloride cushion. The RNA pellet was resuspended in a 7 M urea buffer (7 M urea, 0.5% SDS, 1 mM EDTA, 50 mM Tris-HCl, pH 7.5), then precipitated with ethanol. Twice-selected poly(A) RNA was obtained using an mRNA purification kit (Pharmacia LKB, Piscataway, NJ).

Northern analyses: Poly(A) RNA samples (3 or 5 μg) were electrophoresed in 1.2% agarose, 2.2 M formaldehyde gels for 2–3 hr at 100 V in a 3-(*N*-morpholino) propanesulfonic acid (MOPS)-acetate-EDTA buffer. RNA was then blotted onto Zetabind nylon membrane (Cuno Inc., Meriden, CT) by capillary flow in 20x SSC (AUSUBEL *et al.* 1988). Hybridization and washes were performed according to the method of CHURCH and GILBERT (1984). *Agouti* expression was detected using a cDNA probe containing exons 2–4. Uniformity of loading was checked by hybridization to a chicken *glycerol-3-aldehyde phosphate dehydrogenase* (GAPDH) probe. Comparisons of expression levels were based on densitometry scans of films using an Ultroscan XL Enhanced Laser Densitometer (Pharmacia LKB).

Southern blot analysis: DNA was treated with restriction enzymes obtained from New England Biolabs, Inc. (Boston, MA). Digestion of genomic DNA was as recommended by the manufacturer. Restriction digests were electrophoresed on 0.9% agarose gels and transferred to nylon membranes (Zetabind, Cuno Inc.) as described (JENKINS *et al.* 1982). DNA was cross-linked to the filters by UV irradiation and hybridized to random hexanucleotide-labeled probes (FEINBERG and VOGELSTEIN 1984) described in the text.

RT-PCR analysis: Poly (A)-selected RNA was reverse transcribed using oligo-d(T) and random hexanucleotide primers (Invitrogen, San Diego, CA) and Superscript reverse transcriptase (Bethesda Research Laboratories, Gaithersburg, MD). The cDNA samples from each primer were pooled and amplified by PCR. The resulting PCR products were either sequenced directly (CASANOVA *et al.* 1990) or cloned into PCR-Script vectors (Stratagene, Inc., La Jolla, CA) and then sequenced using Sequenase version 2 (United States Biochemical, Cleveland, OH). Primers were designed based on the cDNA sequence reported by MILLER *et al.* (1993). The primers used for PCR were as follows: primer 5E2 is 5′-GCTTCTCAGGATGGATGTCA-3′, located at the 5′ end of exon 2; and primer 3E4 is 5′-GCAGCCTAAAAATATTATTG-3′, located at the 3′ end of exon 4.

Ligation-anchored PCR analysis: Isolation of the 5′ ends of the *agouti* mRNA was achieved using the method of TROUTT *et al.* (1992). Poly(A)-selected RNA from wild-type C3H/HeJ and mutant mice was reverse transcribed and the resulting cDNA was purified by phenol-chloroform extraction. The cDNA was then ligated to an anchor oligonucleotide (5′-TTTAGTGAGGGTTAATAAGCGGCCGCGTCGACTCTAGAGCGCGA-3′) as described. An aliquot of this ligation reaction was then used in a PCR amplification reaction with the anchor primer (5′-TCTAGAGTCGACGCGGCCGCTTATT-3′) and an *agouti*-specific primer RACE 200 (5′-AGACTCCTGTCATCTCCAAGCGTCT-3′), which spans nucleotides 197–227 of the cDNA (BULTMAN *et al.* 1992; MILLER *et al.* 1993). The

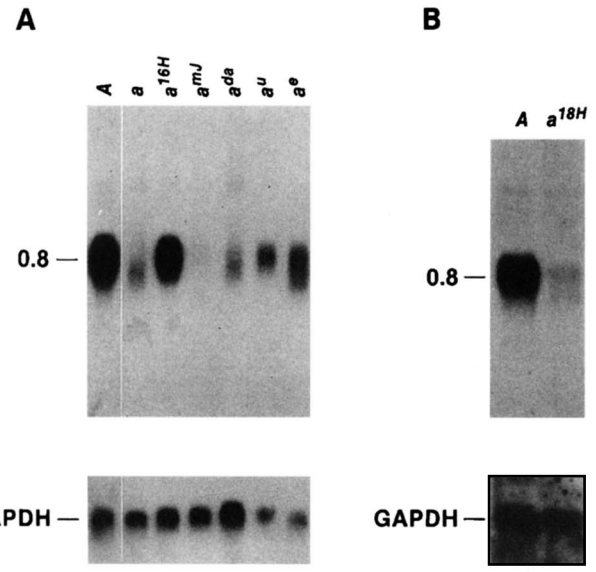

FIGURE 1.—Expression of *agouti* in recessive mutants. (A) Poly(A) RNA (5 μg/lane) from skin of 4–5-day-old homozygous mutant and wild-type (*A*) mice was electrophoresed in a formaldehyde-agarose gel, transferred to a nylon membrane and hybridized to an *agouti* cDNA probe containing exons 2–4. The same filter was then probed with a *GAPDH* cDNA fragment to control for quantity and quality of RNA loaded. Molecular sizes shown are in kilobases. (B) Poly(A) RNA (3 μg/lane) from skin of 4–5-day-old wild-type (*A*) mice and a^{18H} homozygous mutant mice was characterized as described for A.

resulting products were then cloned into PCR-Script vectors (Stratagene Inc.) and sequenced.

Histological analysis: Homozygous and heterozygous a^{18H} mice died or were euthanized and complete necropsies were conducted. Representative tissues were collected and preserved in 10% neutral formalin. Tissues were trimmed, processed, sectioned at ~6-mm thickness and stained with hematoxylin and eosin.

Pulsed-field gel analysis: Spleens from wild-type C3H and a^{18H}/a^{18H} animals were harvested and spleen cells were embedded in 0.5% (w/v) agarose blocks and digested with rare-cutter restriction enzymes as described previously (KINGSLEY *et al.* 1992). Forty-microliter blocks were loaded on a 1% pulsed field gel grade agarose gel and subjected to clamped homogeneous electric field (CHEF) gel electrophoresis (CHU *et al.* 1986) using a CHEF Mapper pulsed field electrophoresis system (Bio-Rad, Melville, NY). Resolution in the size range of 50–1000 kb was achieved using a 50–90-sec pulse for 22 hr at 6 V/cm and 14°. Gels were then UV-nicked and DNA was transferred overnight to Hybond N+ membranes (Amersham, Arlington Heights, IL) by standard alkaline transfer methods. The resulting blots were then treated in the same manner as standard Southern blots.

RESULTS

Six viable recessive *agouti* mutations were analyzed in this study. Two mutations arose spontaneously (a^{mJ}, a^{e}), three were generated by radiation (a^{a}, a^{u}, a^{18H}), and one was generated by treatment with ethylnitrosourea (ENU; a^{16H}; see MATERIALS AND METHODS). The phenotypes of these mice range from nearly agouti to completely black. We determined that the a^{mJ}, a^{da}, a^{u}, a^{18H}, and a^{16H} mutations each arose on a C3H chromosome by using a probe at the *agouti* locus that detected a polymorphism between C3H/HeH or C3H/HeJ, 101/H, and C57BL/6J (see MATERIALS AND METHODS; data not shown). DNA from mice carrying the a^{e} mutation, which arose in the S strain, produced restriction fragments indistinguishable from C3H.

Expression of *agouti*: It would be reasonable to expect that the darker than normal coat colors of some recessive *agouti* mutants might be due to a decrease

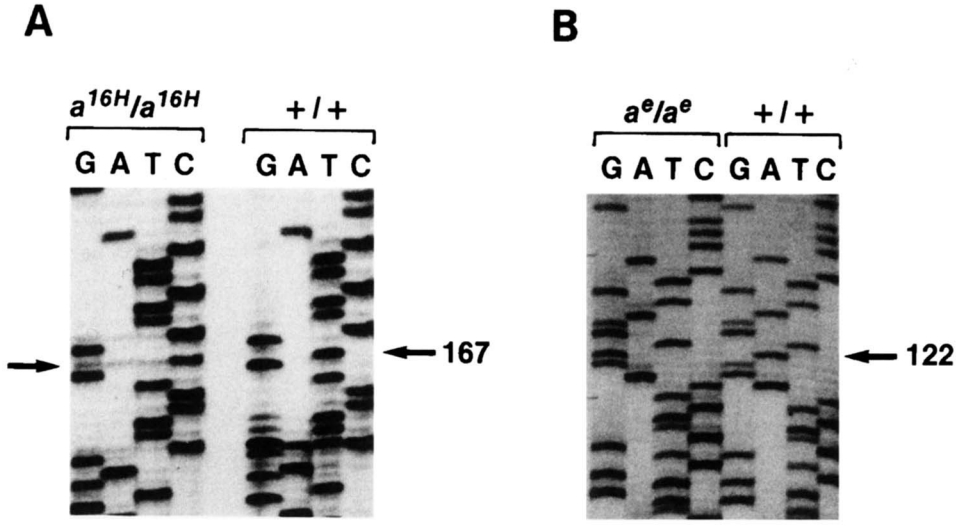

FIGURE 2.—Sequence changes in the *agouti* coding region in a^{16H} and a^{e} mutants. (A) *Agouti* nucleotide sequence from the putative signal peptide region in a^{16H} mutants. RT-PCR was performed using primers that amplify the *agouti* coding region (5E2 and 3E4). The T to C transition at position 167 (arrow) results in a cysteine to arginine change in the amino acid sequence of the mutant. (B) Sequence surrounding the *agouti* translation start site in a^{e} mutants. LA-PCR was performed using a nested anchor primer and an *agouti*-specific primer located near the 3′ end of exon 2 (RACE 200). The A at position 122 in the wild-type sequence (arrow) is deleted in the mutant, destroying the ATG initiation methionine codon.

```
1    GGGCCTCTGGGACGAGTCTGAACCTACTGGGCTGAAAGCAAAGGGGCTTCTCAGGATGGA   60
                                                        M  D      -

61   TGTCACCCGCCTACTCCTGGCCACCCTAGTGAGCTTCCTGTGCTTCTTCACCGTCCACAG  120
      V  T  R  L  L  L  A  T  L  V  S  F  L  C  F  F  T  V  H  S    -

121  CCACCTGGCACTCGAGGAGACGCTTGGAGATGACAGGAGTCTGCGGAGTAACTCCTCCAT  180
      H  L  A  L  E  E  T  L  G  D  D  R  S  L  R  S  N  S  S  M    -

181  GAACTCGCTGGATTTCTCCTCTGTTTCTATCGTGG  215
      N  S  L  D  F  S  S  V  S  I  V      -
```

FIGURE 3.—Sequence of a^{mJ} exon 1. Sequence of the 5′ end of the *agouti* cDNA from a^{mJ} mutants. LA-PCR was performed as in Figure 2B. Instead of one of the known *agouti* exon 1 sequences, a unique 45-bp sequence (nucleotides 1–45) was found spliced to exon 2 (nucleotides 46–215) in a^{mJ} mutants. The amino acid sequence of the open reading frame is shown below the nucleotide sequence.

in the levels of *agouti* mRNA produced in mutants as compared with wild-type mice. To determine if that was the case, poly(A) RNA from skin of 4–5-day-old wild-type C3H/HeJ (*A/A*) and homozygous mutant mice was examined by Northern analysis using an *agouti* cDNA probe (Figure 1, A and B). The a^{16H} and a^{e} mutants show nearly the same level (70%) of *agouti* expression as wild-type C3H mice. The *nonagouti* allele, *a*, shows an eightfold lower level of expression of a smaller *agouti* mRNA; this mutation has recently been determined to be caused by a 12-kb insertion near exon 1C (BULTMAN *et al.* 1992) and is shown here only for comparison with the other recessive mutations. The other mutants show a decreased level of *agouti* message, especially the a^{mJ} and a^{da} mutants (2–3% of wild type).

Analysis of *agouti* genomic alterations: To determine if gross changes in genomic structure could account for the recessive mutant phenotypes, genomic DNA from wild-type and homozygous mutant mice was digested with several enzymes and hybridized to probes essentially covering the entire *agouti* locus. All probes located downstream of exon 1C, including probes containing exon 2, exon 4, and a region just 3′ of the gene, did not detect any alterations in restriction patterns between mutant and wild type (data not shown). Several restriction fragment length polymorphisms (RFLPs) were detected in one of the mutants, a^{da}, when hybridized to a genomic probe, probe 1C, containing both exons 1B and 1C. This alteration has been localized to a region ~5 kb upstream of exon 1B (data not shown; see map in Figure 6A). Because this change is detected in the putative promoter region, this mutation may affect a regulatory element required for normal transcription, resulting in the decreased expression of *agouti* mRNA observed in a^{da} mutants. All other mutants displayed a restriction pattern identical to wild type (data not shown).

TABLE 1

Pathology of a^{18H}/a^{18H} mice on the C57BL/6J background

Tissue	Lesion	No. affected
Lung	Alveolar proteinosis and interstitial inflammation	17/19
Spleen	Hematopoietic cell proliferation	17/20
Lymph nodes	Lymphoid hyperplasia	17/20
Skin/ear	Ulcers, inflammatory processes	14/20
Thymus medulla	Lymphoid hyperplasia	13/16
Forestomach	Epithelial hyperplasia	6/20
Glandular stomach	Inflammation	6/20

Twenty mice were examined (10 males, 10 females) at 4 mo of age.

Sequence analysis of *agouti* transcripts in mutant mice: To test whether mutations in the coding region of *agouti* were responsible for the dark coloration of these recessive mutants, primers from exons 2 and 4 were used in a PCR reaction on reverse-transcribed mRNA from the skin of each mutant strain (RT-PCR). The resulting products were sequenced either directly or after subcloning. Sequencing of the coding region of a^{16H} mutants revealed a point mutation in the putative signal sequence of *agouti* (Figure 2A). This mutation changes the T at position 167 of the cDNA sequence to a C, resulting in a cysteine to arginine change at residue 16 in the amino acid sequence. We confirmed that this base change was a true mutation and not a polymorphism between C3H/HeJ mice, the control used in the RT-PCR reaction, and C3H/HeH mice, on which the mutation arose, by sequencing an exon 2 PCR product from C3H/HeH genomic DNA (Figure 2A). No other coding region mutations were found in any of the other recessive mutants by this method.

To examine the 5′ region of *agouti* for sequence changes, recessive mutant cDNAs were subjected to ligation-anchored PCR (LA-PCR) and then sequenced. Using this technique, mutations were detected in both a^{e} and a^{mJ} animals. Mutant a^{e} animals have a 1-bp deletion

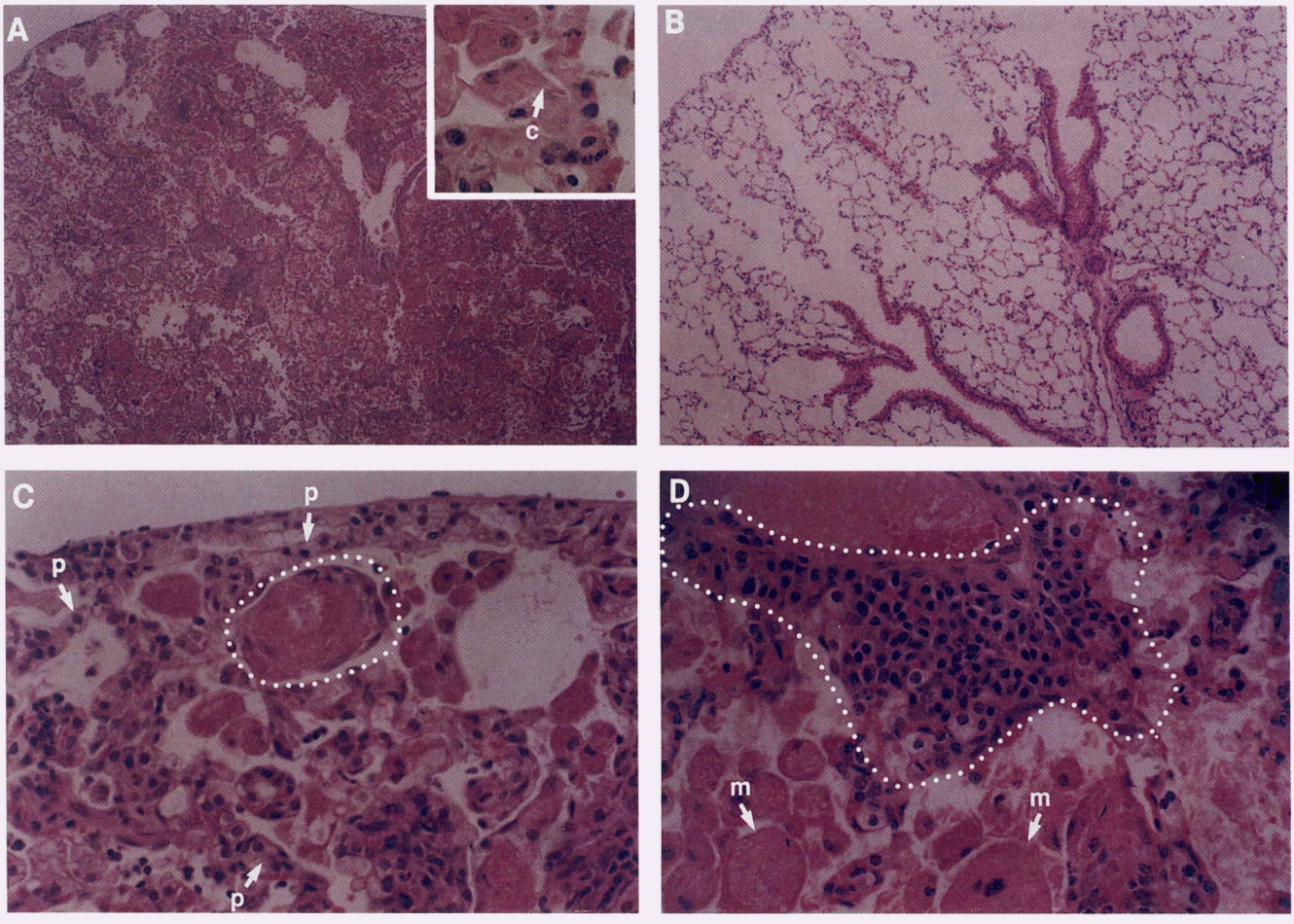

FIGURE 4.—Pathology of lung tissue in a^{18H} homozygotes. Homozygous a^{18H} mice show characteristic lung changes of alveolar proteinosis and chronic interstitial inflammation (A) compared to wild-type mice (B). Airways are laden with macrophages having abundant eosinophilic cytoplasm and cellular debris. (A, inset) shows a macrophage with an intracytoplasmic crystal. (C) Alveoli are lined by type II pneumocytes with numerous clear cytoplasmic vacuoles (p) and organization of exudate is bordered by an aggregate of cellular debris enveloped by epithelial cells and delicate stroma (dashed line). (D) A pulmonary vein is surrounded by a prominent infiltrate of plasma cells (dashed line) with adjacent alveoli laden with macrophages (m). H + E stained sections, magnification, ×48; inset magnification, ×479.

at position 122 of the cDNA, altering the translation start site in exon 2 (Figure 2B). This mutation deletes the A of the ATG initiator methionine, presumably resulting in a lack of translation initiation, and hence no agouti protein. We confirmed the presence of the a^e mutation in genomic DNA by PCR-amplifying exon 2 using genomic primers and sequencing the resulting product. Mutant a^{mJ} animals have a normal coding region, composed of exons 2–4, attached to a new 45-bp sequence at the 5′ end instead of to the wild-type 111-bp exon 1C or other exons 1 (Figure 3). Again, we confirmed that this extra 45 bp of sequence was not due to a PCR artifact by additional independent PCR experiments. Comparison of this 45-bp sequence with others in GenBank does not detect any significant homology to known genes. Hybridization of a probe from this new sequence to genomic clones containing the region upstream of exon 2 has revealed that this sequence is present in a 3-kb region upstream of exon 1B in wild-type animals. Why it is spliced to exon 2 in a^{mJ} animals is unclear. The a^{16H}, a^u and a^{da} mutants do not have any alterations in the 5′ region of the *agouti* cDNA.

Analysis of the a^{18H} mutant: *Nonagouti-*a^{18H} mice are unique among *agouti* mutants, because homozygous a^{18H} mice have an immune disorder as well as a coat-color change. Initial analysis of the a^{18H} mutation was conducted at Harwell in crosses involving inbred JU/Ct-*a*, *c* mice. On this background, homozygous a^{18H} mice became sick at ~3–4 mo and the abdomen was often distended and hard due to a thickening, loss of elasticity, and occasional blockage of the large intestine along all or part of its length. Further examination of these intestinal lesions revealed extensive areas of the submucosa (sub-epithelium) that were infiltrated by inflammatory cells, predominantly polymorphs. At some sites the inflammatory reaction extended into one or both layers of the intestinal wall and contained a higher percentage of mononuclear cells. The above phenotype is consistent with a mouse having an immunological

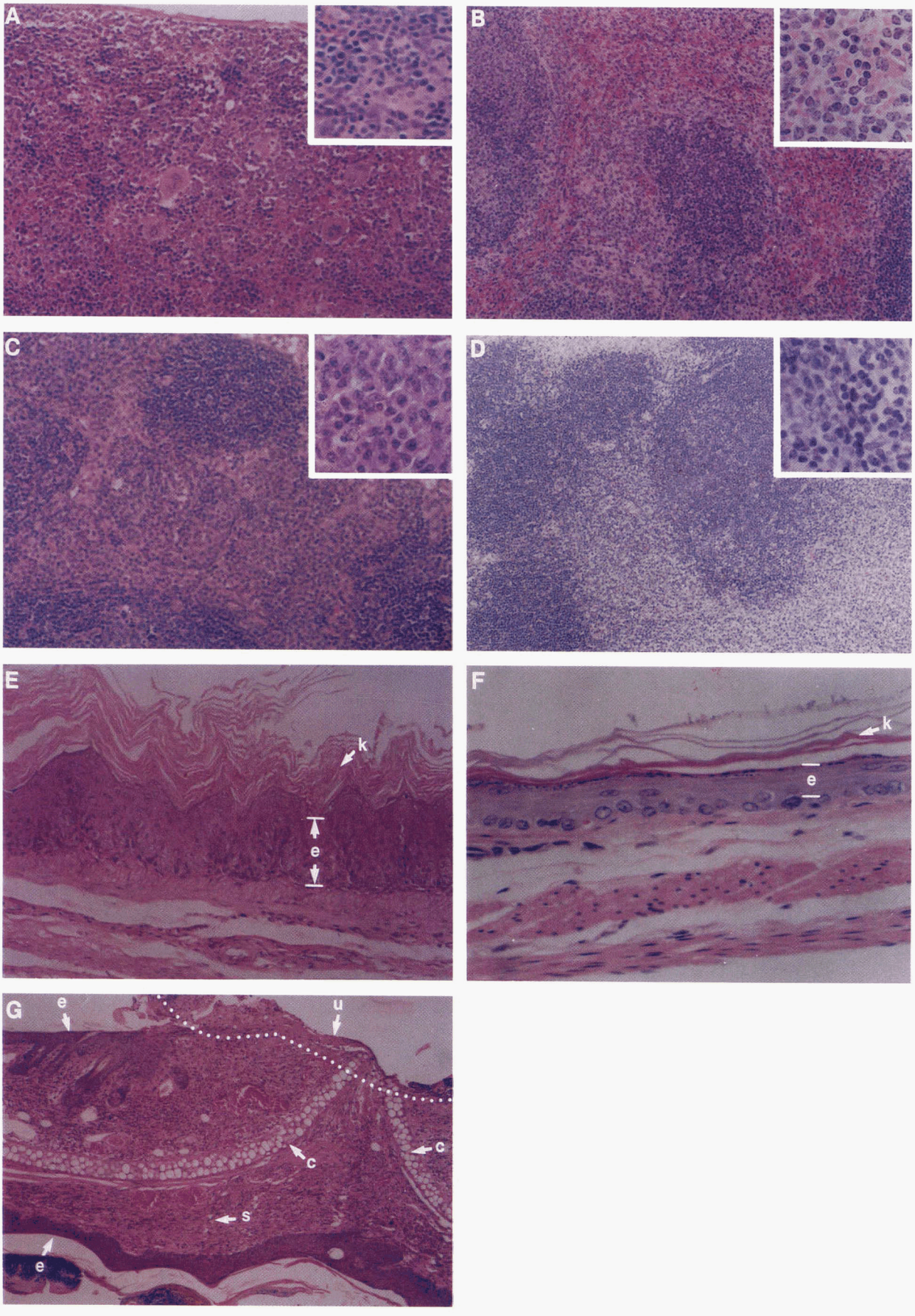
A
B
C
D
E
k
e
F
k
e
G
e
u
c
c
s
e

reaction to the contents of the large intestine. Rarer features included scarring of the skin caused by scratching, primarily affecting the back and regions around the eyes and ears.

Surprisingly, on the C57BL/6J background a^{18H}/a^{18H} mice do not develop any intestinal problems. Instead, homozygous animals exhibit a severe immune disease that results in death at 4–6 mo. A summary of the pathology is given in Table 1. The cause of death of these mice can likely be attributed to hypoxia associated with pulmonary chronic interstitial inflammation and alveolar proteinosis. Lung lesions are characterized by an extensive accumulation of deeply eosinophilic granular or globular material both free in alveoli and within the cytoplasm of macrophages (Figure 4, A and D). Macrophages are large and often multinucleated, and their cytoplasm often appears laminated and infrequently contains large amorphous crystals (Figure 4A, inset). Cells lining alveoli, many considered to be type II pneumocytes, are large and contain clear cytoplasmic vacuoles (Figure 4C). A variable, usually minimal infiltrate of neutrophils in alveoli, perivascular plasma cell infiltrates (Figure 4D), fibrosis of interstitial areas, and organization of exudate in airways resulting in obliterative pneumonia are also seen in the lungs of homozygous mutant animals.

Tissues other than the lung are also affected in a^{18H} homozygous animals. A variable, often marked expansion of the splenic red pulp with hematopoietic cells is frequently observed. Erythroid progenitor cells predominate (Figure 5A), in contrast to the loose reticular stroma and the mixed cell population observed in the red pulp of wild-type animals (Figure 5B). Lymph nodes exhibit hyperplasia of lymphoid follicles and distension of medullary sinusoids with mature plasma cells (Figure 5C). There is a modest hyperplasia of the forestomach epithelium of homozygous mutant mice characterized by an increase in the thickness of the stratified squamous epithelium and a variable hyperkeratosis (Figure 5E). Inflammation of the glandular stomach is observed at low incidence and is characterized by a mixed inflammatory cell infiltrate of the submucosa. A minimal replacement of parietal cells of the glandular epithelium by mucocytes accompanied the inflammatory reaction. The skin of these animals, especially the pinnae of the ear, displays ulcerations, chronic inflammatory processes and epidermal hyperplasia (Figure 5G), presumably due to scratching, as was seen on the JU/Ct-*a*, *c* background. Some heterozygous animals show mild lymphoid hyperplasia in spleen and lymph nodes, but they never exhibit either the lung or skin lesions seen in homozygous a^{18H} animals. The differences in phenotype seen between a^{18H} mice on the JU/Ct-*a*, *c* background and those on the C57BL/6J background may be due to the influences of other genes that modify the effect of the mutation causing immune dysfunction.

Agouti mRNA of normal size is expressed in a^{18H} animals, but at a 10-fold lower level than seen in wild-type C3H animals (Figure 1B). Examination of the coding region including the translation start site as well as the 5′ end of the cDNA by RT-PCR and LA-PCR, respectively, did not detect any sequence changes. Thus, the a^{18H} mutation most likely affects the promoter region of *agouti*, resulting in reduced *agouti* expression.

It is unlikely that the phenotype seen in a^{18H} homozygous mice is due solely to a mutation in the *agouti* gene, because none of the other *agouti* alleles displays an immune disease. Because the a^{18H} mutation likely affects two loci, we would expect a large genomic alteration rather than two separate smaller mutations. To determine if genomic alterations exist near the *agouti* locus, we compared genomic DNA from a^{18H} animals with DNA from the parental strain (C3H/HeH) digested with several restriction enzymes. The blots were hybridized with probes in and near the *agouti* locus (Figure 6A). The only change detected was an increase in the size of a *Kpn*I fragment recognized by an exon 1C-containing probe, from 16 kb in wild-type mice to 16.4 kb in a^{18H} animals (Figure 6B). No changes were detected with probes from the coding region of *agouti* (exon 2 and exon 4) or from the region immediately 3′ of the gene (data not shown). From this we conclude that a mutation associated with the a^{18H} phenotype is upstream of the *agouti* coding region. To further localize the mutation, genomic clones of the 5′ region of *agouti* were isolated using probe 1C. A 1.6-kb *Eco*RI fragment isolated from one of these clones, probe RI-1.6, detects polymorphisms between C3H and a^{18H} DNAs with several enzymes (Figure 6C). In most cases, probe RI-1.6 detects a single band in C3H DNA and two altered bands in a^{18H} DNA, one more intense than the other. This result could be explained if the mutation resulted from an inversion where the breakpoint near the *agouti* locus is located within this 1.6-kb region. Thus part of the

FIGURE 5.—Common lesions in other affected tissues in a^{18H} homozygotes. Splenic red pulp is expanded by a proliferation of hematopoietic cells in mutant (A) versus wild-type (B) animals. The proliferation was composed primarily of erythroid progenitor cells (A, inset) as opposed to loose reticular stroma of the red pulp with the expected lymphoid and hematopoietic cells (B, inset). (C) Mandibular lymph nodes of mutant mice have mild hyperplasia of the follicle and medullary areas are laden with plasma cells (inset) compared to wild-type mandibular lymph nodes (D) showing the expected loose stroma and lymphocyte component (inset). The forestomach of mutant mice (E) shows a hyperplastic stratified squamous epithelium (e) compared to wild-type (F) as well as a thick acellular keratin layer (k). (G) The pinna of the ear in a mutant mouse shows an ulceration of the epithelium (u), exposure of the cartilage (c), chronic inflammation of the subcutis (s) and epithelial hyperplasia (e). H + E stained sections, magnification ×120; inset, magnification ×479; E and F, magnification ×240.

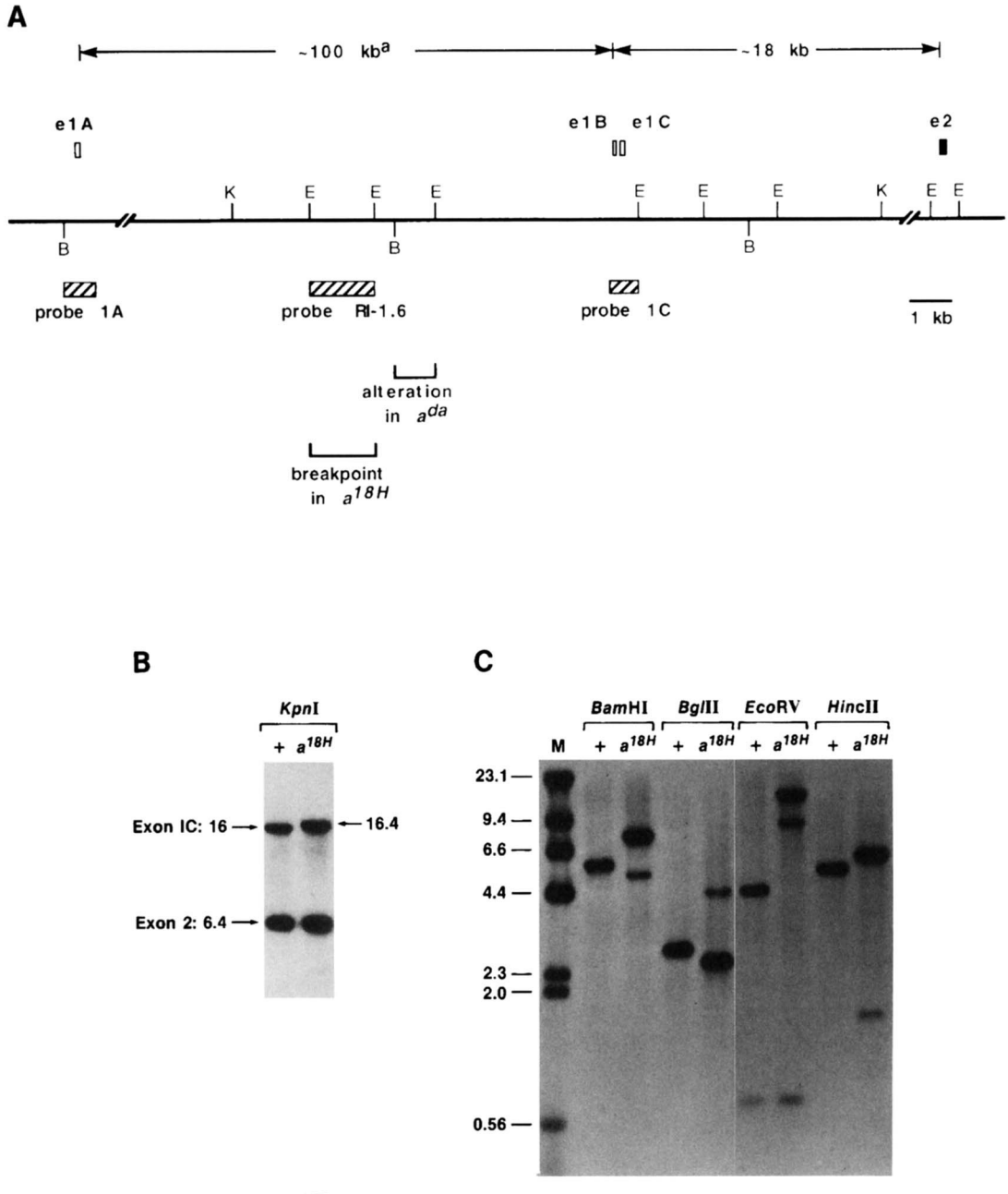

FIGURE 6.—Genomic analysis of the a^{18H} allele. (A) Restriction map of the *agouti* gene showing the locations of *agouti* noncoding exons 1A, 1B and 1C (open boxes) and the first coding exon, exon 2 (solid box). Enzymes used: *Bam*HI, B; *Eco*RI, E; *Kpn*I, K. Probes used in subsequent hybridization analyses (hatched boxes) are designated as probe 1A, a 800-bp *Bam*HI-*Xho*I genomic fragment that contains exon 1A, located ~120 kb upstream of exon 2, the first coding exon; probe RI-1.6, a 1.6-kb *Eco*RI genomic fragment ~25 kb upstream of exon 2; and probe 1C, a 700-bp *Stu*I-*Eco*RI genomic fragment that contains exons 1B and 1C, located ~18 kb upstream of exon 2. [a]Size as reported in VRIELING *et al.* 1994. (B) Comparative Southern analysis of wild type (+/+) and a^{18H}/a^{18H} DNA digested with *Kpn*I and hybridized with a cDNA probe containing exon 1C and 80 bp of exon 2. Because of the large intron between the two exons, two bands are usually detected: the upper band corresponds to the region around exon 1 and the lower band to that around exon 2. Molecular sizes are shown in kilobases. (C) Comparative Southern analysis of wild type (+) and a^{18H}/a^{18H} DNA digested with the indicated enzymes and hybridized with probe RI-1.6. Molecular sizes are shown in kilobases.

probe recognizes one end of the inversion near *agouti,* and the remainder of the probe recognizes the other end of the inversion, presumably near a second locus involved in the immune phenotype of a^{18H} mice.

If an inversion has occurred in a^{18H} mutants, long range restriction analysis may detect differences between C3H and a^{18H} alleles. We used clamped homogeneous electric field (CHEF) gel electrophoresis to show large RFLPs between a^{18H} and C3H DNAs (Figure 7, A and B). No changes between the *Bss*HII and *Eag*I restriction patterns of C3H and a^{18H} DNAs were detected with an exon 4 probe or with a probe just 3′ of

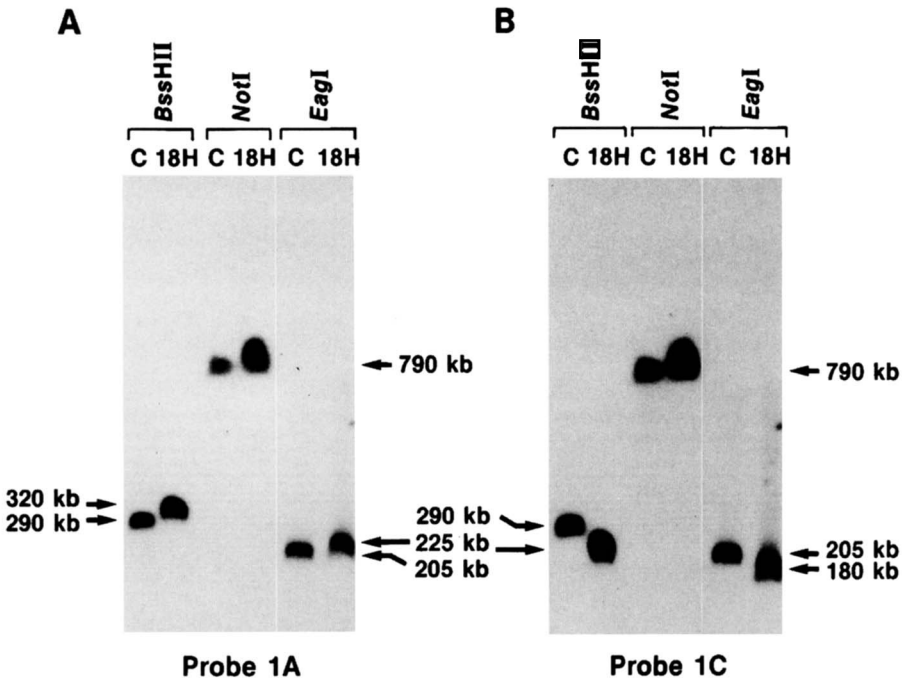

FIGURE 7.—Pulsed field gel analysis of the a^{18H} allele. Spleen DNA samples from C3H/OR and a^{18H} homozygotes were digested with *Bss*HII (B), *Eag*I (E), or *Not*I (N), separated by CHEF electrophoresis, and analyzed by blot hybridization with probe 1A (A) or probe 1C (B). The *Not*I fragment is the same size (790 kb) in both mutant and control with both probes 1A and 1C. The sizes of the *Bss*HII and *Eag*I bands in the controls probed with 1A are the same size (290 and 205 kb, respectively) as those probed with 1C. The sizes of the mutant *Bss*HII and *Eag*I bands detected with probe 1A are different than those detected with probe 1C.

the *agouti* gene, providing further evidence that the mutation in a^{18H} occurs near the 5′ end of the *agouti* gene (data not shown). A 790-kb *Not*I fragment is detected in C3H and a^{18H} DNA with both probe 1A (Figure 7A) and probe 1C (Figure 7B), and changes that occur within this fragment are probably responsible for the mutant phenotype. Specifically, a 290-kb *Bss*HII band is detected by probes 1A and 1C in C3H DNA, but 320- and 225-kb *Bss*HII bands are detected in a^{18H} DNA with probes 1A and 1C, respectively. Similarly, both probes detect a 205-kb *Eag*I band in C3H DNA, but 225- and 180-kb *Eag*I bands are detected in mutant DNA with probes 1A and 1C, respectively. These results suggest that the a^{18H} mutation did not arise from a simple deletion.

More direct evidence that a^{18H} results from an inversion comes from physical analysis of a mouse yeast artificial chromosome (YAC) that we have isolated with probes from the *agouti* region (LEHRACH *et al.* 1990). CHEF analysis indicates that the *agouti* coding region on this YAC (YLE1130) maps ~180 kb from the right arm. Interestingly, a probe isolated from the proximal side of the a^{18H} breakpoint near *agouti* exon 1B maps on the opposite side of *agouti* on this YAC (near the right arm) as a probe from *Raly*, a locus encoding an RNA-binding protein that has been localized ~280 kb proximal of *agouti* in wild-type DNA (DUHL *et al.* 1994a; MICHAUD *et al.* 1994a). Because the breakpoint probe was isolated from a region that maps proximal of *agouti* in a^{18H} DNA, but maps downstream of *agouti* in wild-type YAC DNA, the rearrangement in a^{18H} must, at least in part, result from an inversion. The location of the *agouti* breakpoint probe on wild-type YAC DNA suggests that the distal breakpoint of the inversion lies within a region no more than 180 kb distal of *agouti* (data not shown).

DISCUSSION

We have examined the structure of the *agouti* locus in six recessive viable mutations to identify alterations that might be responsible for the phenotypes exhibited by these mice. Results are summarized in Table 2. Four of the six mutations (a^{mJ}, a^{u}, a^{da} and a^{18H}) appear to be regulatory mutations that affect the expression of *agouti* mRNA. The other two recessive mutations (a^{16H} and a^{e}) affect the coding region. *Nonagouti-16H* mice were found to have a T to C transition at position 167 in the putative signal sequence of the *agouti* gene. This change results in a cysteine to arginine substitution at residue 16 of the protein. Because the level of *agouti* mRNA produced by these mice is near normal, this mutation is likely to be acting at the level of the protein. The change from an uncharged polar amino acid (cysteine) to a charged amino acid (arginine) may interfere with the structure of the signal sequence, preventing the agouti protein from being correctly transported and secreted into the hair follicle. Similar mutations in bacteria (OLIVER 1985) and yeast (KAISER and BOTSTEIN 1986) have been shown to greatly impair, but not prevent, protein secretion. *Extreme nonagouti* mice were found to have a point mutation that deletes the A of the ATG in the translation start site at position 122 of the cDNA sequence. This deletion should prevent the agouti protein from being expressed, which in turn, would produce the eumelanotic phenotype seen in a^{e} mice.

Given the large and genetically complex promoter

TABLE 2

Analysis of recessive *agouti* mutants

agouti mutant	Mutation induction	*agouti* expression	Genomic alteration[a]	cDNA sequence difference[b]	Nature of mutation
a^{mj}	Spontaneous	Decreased	No	Yes	New exon 1
a^{u}	Radiation	Decreased	No	No	Promoter/regulatory
a^{18H}	Chem + rad	Decreased	Yes	No	Promoter/regulatory
a^{16H}	ENU[c]	Normal	No	Yes	TGC(Cys) to CGC(Arg)
a^{da}	Radiation	Decreased	Yes	No	Promoter/regulatory
a^{e}	Radiation	Normal	No	Yes	No initiation

[a] Southern blots of *Kpn*I-digested (a^{18H}) or *Bam*HI-digested C3H and mutant DNAs were hybridized to an *agouti* cDNA probe containing exon 1C and 80 bp of exon 2.

[b] Mutations in the coding region were determined using reverse transcriptase-PCR (RT-PCR). Mutations in the 5′ region were determined using ligation-anchored PCR (LA-PCR). PCR products were either sequenced directly or subcloned into PCR-Script vectors and then sequenced.

[c] Ethylnitrosourea.

region of *agouti* compared with the small coding region, it is not surprising that most of the mutations described to date, both dominant and recessive, are regulatory. Multiple isoforms of the *agouti* mRNA have been described (VRIELING *et al.* 1994), but the temporal and spatial expression patterns of each isoform have not been completely elucidated. There may be some elements, as yet unidentified, which modulate usage of the various untranslated exons in specific parts of the body. Variations in the phenotypes of the recessive regulatory mutants described here may be due to mutations in elements necessary for proper expression from either the hair-cycle specific exons or the ventral-specific exons or both.

The two phenotypes associated with the a^{18H} mutation are probably the result of an inversion that affects two loci: *agouti* and another, as yet unidentified, gene that maps within 180 kb distal of *agouti*. The proximal breakpoint, located ~6 kb upstream of *agouti* exon 1B, has been cloned. Studies are underway to determine the exact location of the second distal breakpoint. Although the *Ahcy* gene, which has been implicated in the prenatal lethality associated with the a^{x} mutation (MILLER *et al.* 1994), is predicted to be contained within the inverted sequence, the a^{18H} inversion is not likely to affect *Ahcy* expression, as no prenatal lethality is associated with the a^{18H} phenotype.

The disease phenotype exhibited by a^{18H} mice is similar to that of another recessive mutation, *motheaten*. There are two alleles of this locus: *motheaten* (*me*), causing death in the homozygous condition at 6–8 weeks (GREEN and SHULTZ 1975; SIDMAN *et al.* 1978), and *motheaten viable* (me^{v}), causing death at ~25 weeks of age (SHULTZ *et al.* 1984). This mutation is characterized by early onset autoimmunity and severe immunodeficiency, also seen in a^{18H} mice. The cause of death in both *motheaten* and a^{18H} mice, as well as the pathology of the lungs, lymph nodes, and spleens of both mutants, is quite similar, varying mainly in degree of severity. The lungs of both mutants have macrophages with eosinophilic granular cytoplasm containing intracellular crystals, but the number of crystals is greater in *motheaten* mice (WARD 1978). The skin of *motheaten* mice has neutrophilic lesions in the epidermis that disrupt hair follicles and pigmentation and is responsible for their patchy appearance, hence the naming of this mutant. The skin of some a^{18H} mutant mice (14/20 autopsied) show ulcerations and chronic inflammatory processes, but not the pronounced neutrophilia seen in the *motheaten* mutants. There are three differences in the tissues affected in a^{18H} and *motheaten* mice. One feature seen in a^{18H} mice that is not present in *motheaten* animals is a hyperplasia of the forestomach and occasional inflammation of the glandular stomach. Also, the kidneys of *motheaten* mutants exhibit granular deposits of immunoglobulins in glomeruli, evidence of a severe autoimmune defect; only three a^{18H} mice had any glomerulopathy. Additionally, me^{v}/me^{v} mice are sterile, while a^{18H} mice are fertile.

The gene mutated in *motheaten* mice has been cloned (YI *et al.* 1992). Point mutations in the *hematopoietic cell phosphatase* (*Hcph*) gene on the distal end of chromosome 6 are seen in both *me* and me^{v} animals (SHULTZ *et al.* 1993; TSUI *et al.* 1993). It is possible that the second locus disrupted in a^{18H} mutants may be part of the same pathway as HCP or may play a role in a related pathway. Cloning of the gene disrupted by the putative inversion in a^{18H} mice is underway and should allow us to test this hypothesis.

We thank G. BARSH for kindly providing probes 1A and 1C. We also thank D. A. SWING and J. DIETZ for mouse room support, N. O'SULLIVAN for technical support, and E. STEINGRIMSSON and C. BRANNAN for critical reading of the manuscript. This work was supported in part by the National Cancer Institute, Department of Health and Human Services, under contract NO1-CO-46000 with ABL.

LITERATURE CITED

AUSUBEL, F. M., R. BRENT, R. E. KINGSTON, D. D. MOORE, J. G. SEIDMAN *et al.*, 1988 *Current Protocols in Molecular Biology*. John Wiley & Sons, New York.

BULTMAN, S. J., E. J. MICHAUD and R. P. WOYCHIK, 1992 Molecular characterization of the mouse *agouti* locus. Cell **71:** 1195–1204.

BULTMAN, S. J., M. L. KLEBIG, E. J. MICHAUD, H. O. SWEET, M. T. DAVISSON *et al.*, 1994 Molecular analysis of reverse mutations from nonagouti (*a*) to black-and-tan (a^t) and white-bellied agouti (A^w) reveals alternative forms of agouti transcripts. Genes Dev. **8:** 481–490.

CASANOVA, J.-L., C. PANNETIER, C. JAULIN and P. KOURILSKY, 1990 Optimal conditions for directly sequencing double-stranded PCR products with Sequenase. Nucleic Acids Res. **18:** 4028.

CATTANACH, B. M., M. F. LYON, J. PETERS and A. G. SEARLE, 1987 *Agouti* locus mutations at Harwell. Mouse News Lett. **77:** 123–125.

CHIRGWIN, J. M., A. E. PRZYBYLA, R. J. MACDONALD and W. J. RUTTER, 1979 Isolation of biologically active ribonucleic acid from sources enriched in ribonuclease. Biochemistry **18:** 5294–5299.

CHU, G., D. VALLRATH and R. W. DAVIS, 1986 Separation of large DNA molecules by contour-clamped homogeneous electric fields. Science **234:** 1582–1585.

CHURCH, G. M., and W. GILBERT, 1984 Genomic sequencing. Proc. Natl. Acad. Sci. USA **81:** 1991–1995.

COLEMAN, D. L., 1982 Diabetes-obesity syndromes, pp. 125–132 in *The Mouse in Biomedical Research IV,* edited by H. L. FOSTER, J. D. SMALL and J. G. FOX. Academic Press, New York.

DICKIE, M. M., 1969 Mutations at the *agouti* locus in the mouse. J. Hered. **60:** 20–25.

DUHL, D. M. J., M. E. STEVENS, H. VRIELING, P. J. SAXON, M. W. MILLER *et al.* 1994a Pleiotropic effects of the mouse *lethal yellow* (A^y) mutation explained by deletion of a maternally expressed gene and the simultaneous production of *agouti* fusion RNAs. Development **120:** 1695–1708.

DUHL, D. M. J., H. VRIELING, K. A. MILLER, G. L. WOLFF and G. S. BARSH, 1994b Neomorphic *agouti* mutations in obese yellow mice. Nat. Genet. **8:** 59–65.

FEINBERG, A. P., and B. VOGELSTEIN, 1984 A technique for radiolabeling DNA restriction fragments to high specific activity. Anal. Biochem. **137:** 266–267.

FRIGERI, L. G., G. L. WOLFF and C. TEGUH, 1988 Differential responses of yellow A^w/A and agouti A/a (BALB/c × VY) F1 hybrid mice to the same diets: glucose tolerance, weight gain, and adipocyte cellularity. Int. J. Obes. **12:** 305–320.

GREEN, M. C., 1989 Catalog of mutant genes and polymorphic loci, pp. 17–20 in *Genetic Variants and Strains of the Laboratory Mouse,* edited by M. F. LYON and A. G. SEARLE. Oxford University Press, Oxford, UK.

GREEN, M. C., and L. D. SHULTZ, 1975 *Motheaten,* an immunodeficient mutant of the mouse. I. Genetics and pathology. J. Hered. **66:** 250–258.

HELLERSTRÖM, C., and B. HELLMAN, 1963 The islets of Langerhans in yellow obese mice. Metabolism **12:** 527–536.

HESTON, W. E., and G. VLAHAKIS, 1961 Influences of the A^y gene on mammary-gland tumors, hepatomas, and normal growth in mice. J. Natl. Cancer Inst. **26:** 969–982.

HESTON, W. E., and G. VLAHAKIS, 1968 C3H-A^w- a high hepatoma and high mammary tumor strain of mice. J. Natl. Cancer Inst. **40:** 1161–1166.

HOLLANDER, W. F., and J. W. GOWEN, 1956 An extreme nonagouti mutant in the mouse. J. Hered. **47:** 221–224.

JENKINS, N. A., N. G. COPELAND, B. A. TAYLOR and B. K. LEE, 1982 Organization, distribution, and stability of endogenous ecotropic murine leukemia virus DNA sequences in chromosomes of *Mus musculus.* J. Virol. **43:** 26–36.

KAISER, C. A., and D. BOTSTEIN, 1986 Secretion-defective mutations in the signal sequence for *Saccharomyces cerevisiae* invertase. Mol. Cell. Biol **6:** 2382–2391.

KINGSLEY, D. M., A. E. BLAND, J. M. GRUBBER, P. C. MARKER, L. B. RUSSELL *et al.*, 1992 The mouse *short ear* skeletal morphogenesis locus is associated with defects in a bone morphogenetic member of the TGFβ superfamily. Cell **71:** 399–410.

LEHRACH, H., R. DRMANAC, J. HOHEISEL, Z. LARIN, G. LENNON *et al.*, 1990 Hybridization fingerpainting in genome mapping and sequencing, pp. 39–81 in *Genome Analysis Volume 1: Genetic and Physical Mapping,* edited by K. E. DAVIES and S. M. TILGHMAN. Cold Spring Harbor Laboratory Press, Cold Spring Harbor, NY.

LYON, M. F., G. FISHER and P. H. GLENISTER, 1985 A recessive allele of the mouse *agouti* locus showing lethality with yellow, A^y. Genet. Res. **46:** 95–99.

MICHAUD, E. J., S. J. BULTMAN, L. J. STUBBS and R. P. WOYCHIK, 1993 The embryonic lethality of homozygous lethal yellow mice (A^y/A^y) is associated with the disruption of a novel RNA-binding protein. Genes Dev. **7:** 1203–1213.

MICHAUD, E. J., S. J. BULTMAN, M. KLEBIG, M. VAN VUGT, L. STUBBS *et al.*, 1994a A molecular model for the genetic and phenotypic characteristics of the mouse lethal yellow (A^y) mutation. Proc. Natl. Acad. Sci. USA **91:** 2562–2566.

MICHAUD, E. J., M. J. VAN VUGT, S. J. BULTMAN, H. O. SWEET, M. T. DAVISSON *et al.*, 1994b Differential expression of a new dominant *agouti* allele (A^{iapy}) is correlated with methylation state and is influenced by parental lineage. Genes Dev. **8:** 1463–1472.

MILLER, M. W., D. M. J. DUHL, H. VRIELING, S. P. CORDES, M. M. OLLMANN *et al.*, 1993 Cloning of the mouse *agouti* gene predicts a secreted protein ubiquitously expressed in mice carrying the *lethal yellow* mutation. Genes Dev. **7:** 454–467.

MILLER, M. W., D. M. J. DUHL, B. M. WINKES, F. ARREDONDO-VEGA, P. J. SAXON *et al.*, 1994 The mouse *lethal nonagouti* (a^x) mutation deletes the *S-adenosylhomocysteine hydrolase* (*Ahcy*) gene. EMBO J. **13:** 1806–1816.

OLIVER, D., 1985 Protein secretion in *Escherichia coli.* Annu. Rev. Microbiol. **39:** 615–648.

PHILLIPS, R. J. S., 1959 Agouti-umbrous (Abstr.). Mouse News Lett. **21:** 39.

PHILLIPS, R. J. S., 1976 New A-alleles (Abstr.). Mouse News Lett. **55:** 14.

SAMBROOK, J., E. F. FRITSCH and T. MANIATIS, 1989 *Molecular Cloning: A Laboratory Manual.* Cold Spring Harbor Laboratory Press, Cold Spring Harbor, NY.

SHULTZ, L. D., D. R. COMAN, C. L. BAILEY, W. G. BEAMER and C. L. SIDMAN, 1984 "Viable motheaten", a new allele at the *Motheaten* locus. I. Pathology. Am. J. Pathol. **116:** 179–192.

SHULTZ, L. D., P. A. SCHWEITZER, T. V. RAJAN, T. YI, J. N. IHLE *et al.*, 1993 Mutations at the murine motheaten locus are within the hematopoietic cell protein-tyrosine phosphatase (*Hcph*) gene. Cell **73:** 1445–1454.

SIDMAN, C. L., L. D. SHULTZ and E. R. UNANUE, 1978 The mouse mutant "motheaten". I. Development of lymphocyte populations. J. Immunol. **121:** 2392–2398.

SIRACUSA, L. D., 1994 The *agouti* gene: turned on to yellow. Trends Genet. **10:** 423–428.

SILVERS, W. K., 1979 The *agouti* and *extension* series of alleles, umbrous, and sable, pp. 6–44 in *The Coat Color of Mice. A Model for Mammalian Gene Action and Interaction.* Springer-Verlag, New York.

TROUTT, A. B., M. G. MCHEYZER-WILLIAMS, B. PULENDRAN and G. J. V. NOSSAL, 1992 Ligation-anchored PCR: a simple amplification technique with single-sided specificity. Proc. Natl. Acad. Sci. USA **89:** 9823–9825.

TSUI, H. W., K. A. SIMINOVITCH, L. DE SOUZA and F. W. L. TSUI, 1993 *Motheaten* and *viable motheaten* mice have mutations in the haematopoietic cell phosphatase gene. Nat. Genet. **4:** 124–129.

VRIELING, H., D. M. J. DUHL, S. E. MILLAR, K. A. MILLER and G. S. BARSH, 1994 Differences in dorsal and ventral pigmentation result from regional expression of the mouse *agouti* gene. Proc. Natl. Acad. Sci. USA **91:** 5667–5671.

WARD, J. M., 1978 Pulmonary pathology of the motheaten mouse. Vet. Pathol. **15:** 170–178.

YEN, T. T., A. M. GILL, L. G. FRIGERI, G. S. BARSH and G. L. WOLFF, 1994 Obesity, diabetes, and neoplasia in yellow A^w/- mice; ectopic expression of the *agouti* gene. FASEB J. **8:** 479–488.

YI, T., J. L. CLEVELAND and J. N. IHLE, 1992 Protein tyrosine phosphatase containing SH2 domains: characterization, preferential expression in hematopoietic cells, and localization to human chromosome 12p12-p13. Mol. Cell. Biol. **12:** 836–846.

Communicating editor: R. E. GANSCHOW